doi:10.1093/jmcb/mjy054
Published online October 9, 2018

Article

Esrrb plays important roles in maintaining self-renewal of trophoblast stem cells (TSCs) and reprogramming somatic cells to induced TSCs

Haibo Gao[2,†], Rui Gao[1,†], Linfeng Zhang[1,†], Wenchao Xiu[1], Ruge Zang[1], Hong Wang[1], Yong Zhang[1], Jiayu Chen[1,*], Yawei Gao[1,*], and Shaorong Gao[1,*]

[1] Clinical and Translational Research Center of Shanghai First Maternity and Infant Hospital, Shanghai Key Laboratory of Signaling and Disease Research, School of Life Sciences and Technology, Tongji University, Shanghai 200092, China
[2] Peking University-Tsinghua University-National Institute of Biological Sciences Joint Graduate Program, School of Life Sciences, Tsinghua University, Beijing 100084, China
[†] These authors contributed equally to this work.
[*] Correspondence to: Shaorong Gao, E-mail: gaoshaorong@tongji.edu.cn; Yawei Gao, E-mail: gaoyawei@tongji.edu.cn; Jiayu Chen, E-mail: chenjiayu@tongji.edu.cn

Edited by Qi Zhou

Trophoblast stem cells (TSCs), which can be derived from the trophoectoderm of a blastocyst, have the ability to sustain self-renewal and differentiate into various placental trophoblast cell types. Meanwhile, essential insights into the molecular mechanisms controlling the placental development can be gained by using TSCs as the cell model. *Esrrb* is a transcription factor that has been shown to play pivotal roles in both embryonic stem cell (ESC) and TSC, but the precise mechanism whereby Esrrb regulates TSC-specific transcriptome during differentiation and reprogramming is still largely unknown. In the present study, we elucidate the function of Esrrb in self-renewal and differentiation of TSCs, as well as during the induced TSC (iTSC) reprogramming. We demonstrate that the precise level of *Esrrb* is critical for stem state maintenance and further trophoblast differentiation of TSCs, as ectopically expressed *Esrrb* can partially block the rapid differentiation of TSCs in the absence of fibroblast growth factor 4. However, *Esrrb* depletion results in downregulation of certain key TSC-specific transcription factors, consequently causing a rapid differentiation of TSCs and these *Esrrb*-deficient TSCs lose the ability of hemorrhagic lesion formation *in vivo*. This function of Esrrb is exerted by directly binding and activating a core set of TSC-specific target genes including *Cdx2, Eomes*, *Sox2, Fgfr4*, *and Bmp4*. Furthermore, we show that *Esrrb* overexpression can facilitate the MEF-to-iTSC conversion. Moreover, *Esrrb* can substitute for *Eomes* to generate GEsTM-iTSCs. Thus, our findings provide a better understanding of the molecular mechanism of Esrrb in maintaining TSC self-renewal and during iTSC reprogramming.

Keywords: Esrrb, trophoblast stem cell, self-renewal, differentiation, iTSC reprogramming

Introduction

Trophoblast stem cells (TSCs), which can be derived from the trophectoderm of a blastocyst following the first cell fate determination or from the extra-embryonic ectoderm on embryonic day 6.5 (E6.5), can sustain self-renew *in vitro* and further contribute to placenta development *in vivo*. Besides, TSCs can generate extra-embryonic lineages and differentiate into various trophoblast cell types including spongiotrophoblast, labyrinth, syncytiotrophoblast, as well as trophoblast giant cells (TGCs) (Tanaka et al., 1998; Cockburn and Rossant, 2010; Roberts and Fisher, 2011; Adachi et al., 2013). Mouse TSC has been well established for about 20 years, which is identified as a good cell model to gain insight into the molecular mechanism controlling the placental development (Tanaka et al., 1998; Latos and Hemberger, 2014), while isolation of human TSCs was not achieved until recently (Okae et al., 2018). In addition, mouse TSCs have been used to aggregate with embryonic stem cells (ESCs) so as to generate artificial embryos, which has the great differentiation potential and can generate *Stella*-positive primordial germ cells (PGCs) (Sozen et al., 2018).

Similar to canonical mouse ESCs that are derived from inner cell mass, TSCs are permanent and can self-renew when they are maintained in stem cell condition by appropriate signals. For

Received May 17, 2018. Revised August 19, 2018. Accepted October 9, 2018.

example, fibroblast growth factor (Fgf) signaling can predominantly activate the Mek/Erk pathway, thus leading to the expression of essential TSC-specific transcription factors (TFs), which are critical to maintain its stem state (Tanaka et al., 1998; Kunath et al., 2004; Ralston and Rossant, 2006; Latos and Hemberger, 2014). However, withdrawal of fibroblast growth factor 4 (Fgf4) in the culture condition results in a rapid differentiation of TSCs. Thus, the property of TSCs to preserve the trophoblast-specific feature as well as the expression of stage- and cell type-specific markers after proper signaling stimulation, provides an important system to investigate both the critical TFs and signals during early trophoblast development.

A number of TFs including caudal-type homeobox factor *Cdx2* (Strumpf et al., 2005), T-box gene *Eomes* (Russ et al., 2000), Ets family member *Elf5* (Donnison et al., 2005), Gata motif-containing factor *Gata3* (Ralston et al., 2010), AP-2 family Member *Tfap2c* (Auman et al., 2002; Werling and Schorle, 2002), Ets family member *Ets2* (Yamamoto et al., 1998; Georgiades and Rossant, 2006; Wen et al., 2007; Odiatis and Georgiades, 2010), estrogen-related receptor *Esrrb* (Adachi et al., 2013; Latos et al., 2015), and SRY-box gene *Sox2* (Adachi et al., 2013) have been proved to be critical for the establishment and/or maintenance of TSC properties. Recent findings have suggested that Esrrb is a downstream target of Fgf signaling specifically in TSC and is pivotal to drive TSC self-renewal (Adachi et al., 2013; Latos et al., 2015). In addition, combined expression of *Sox2* and *Esrrb* can sustain the self-renewal of TSCs in the absence of Fgf4 (Adachi et al., 2013). Moreover, *Esrrb* knockout may cause embryonic lethal at ~E10.5 due to the severe defects in trophoblast development (Luo et al., 1997). Besides, TSCs cannot be successfully derived when *Esrrb* was fully depleted (Tremblay et al., 2001). However, the underlying mechanism whether and how Esrrb regulates TSC-specific transcriptome during differentiation as well as reprogramming still remains elusive.

Mouse embryonic and extra-embryonic lineages are strictly separated by a distinct epigenetic barrier. For example, H3K9me3 and H3K27me3 showed great differences between these two lineages in E6.5–E7.5 embryos (Cambuli et al., 2014; Wang et al., 2018). However, manipulation of a single lineage-determining TF, *Oct4*, is sufficient to reprogram TSCs towards pluripotent state and generates O-iPSCs with germline transmission abilities (Wu et al., 2011). Additionally, recent studies have shown that transient overexpression of *Tfap2c*, *Gata3*, *Eomes*, and *c-Myc* or *Ets2* is sufficient to reprogram mouse embryonic fibroblasts (MEFs) into induced TSCs (iTSCs) (Benchetrit et al., 2015; Kubaczka et al., 2015). These findings indicated that the epigenetic barrier between embryonic and extra-embryonic lineages can be overcome by activating proper core TFs and/or signals.

Here, we elucidate the function of Esrrb in TSC stem state maintaining, differentiation, as well as during iTSC reprogramming. We show that Esrrb is a pivotal regulator in the transcriptional network of TSC, and forced expression of *Esrrb* alone can partially block the rapid differentiation of TSCs in the absence of Fgf4. However, depletion of *Esrrb* results in downregulation of key TSC-specific TFs, consequently leading to *in vitro* differentiation and loss of the hemorrhagic lesion formation ability when subcutaneously injected into the immune-deficient nude mice. This function of Esrrb is realized by directly binding and activating a core set of TSC-specific genes and signals including *Cdx2*, *Eomes*, *Sox2*, *BMP4*, and *Fgfr4*. Besides, we further demonstrate that Esrrb can facilitate the conversion of iTSCs from MEFs. In addition, *Esrrb* can substitute for *Eomes* and initiate iTSC reprogramming along with *Gata3*, *Tfap2c*, and *c-Myc*.

Results

Esrrb is critical for proper proliferation and differentiation of TSCs

To explore which TF may govern the core regulatory network of TSC, we performed a gene knockdown (KD) assay in TSCs cultured under stem state condition (Latos and Hemberger, 2014). The TSCs were stably infected with lentivirus carrying shRNAs directed against several selected TSC-related TFs (shTF-1 or shTF-2), while the scrambled shRNA was set as a control (shControl) (Figure 1A and Supplementary Figure S1A). Among those candidates, we identified that depletion of *Esrrb*, *Tfap2c*, *Gata3*, or *Sox2* triggered a more obvious differentiation phenotype (Supplementary Figure S1B). Quantitative analysis demonstrated that TFs implicated in TSC maintenance including *Cdx2*, *Eomes*, and *Elf5* were dramatically downregulated in *Esrrb*-KD experiments (Figure 1A). Moreover, *Esrrb*-KD led to a remarkable decreased proliferation rate which was similar to that observed in lack of Fgf4 (Figure 1B). In addition, the Cdx2 protein level was significantly downregulated despite the presence of Fgf4 in the culture condition (Figure 1C and Supplementary Figure S1C).

It is known that deprivation of Fgf4 would result in rapid differentiation of TSCs, which was confirmed by downregulation of prominent TSC markers, concomitant with upregulation of genes associated with trophoblast differentiation, including *Gcm1*, *Mash2*, *Tpbpa*, *Pl1*, and *Pl2* (Supplementary Figure S1D). Intriguingly, depletion of *Esrrb* presented a more similar phenotype even with Fgf4 addition, which further triggered the TSCs exiting from stem-like population and primed these cells to differentiate into TGCs (Supplementary Figure S1B and D). We further investigated the *in vivo* differentiation potential of these TSCs. The control and *Esrrb*-KD TSCs were separately subcutaneously injected into the immune-deficient nude mice. Hematoxylin–eosin (H&E) analysis clearly indicated that *Esrrb* depletion restricted the invasion and differentiation abilities of TSCs *in vivo*, which formed a smaller hemorrhagic lesion with limited trophoblast cell types as compared to that of wild-type TSCs (Figure 1D). Eight-cell stage embryo injection assay further confirmed that the *Esrrb*-KD TSCs showed a reduced *in vivo* chimeric ability (Supplementary Figure S1E and F). Above all, these results identify *Esrrb* as a critical TF in regulating self-renewal, proliferation, as well as *in vivo* and *in vitro* differentiation of TSCs.

Forced expression of Esrrb keeps TSCs in a stem-like state in the absence of Fgf4

To further evaluate the functional roles of Esrrb in Fgf signaling in TSCs, we used a gain-of-function approach to test whether the requirement of Fgf4 in TSC culture condition can be

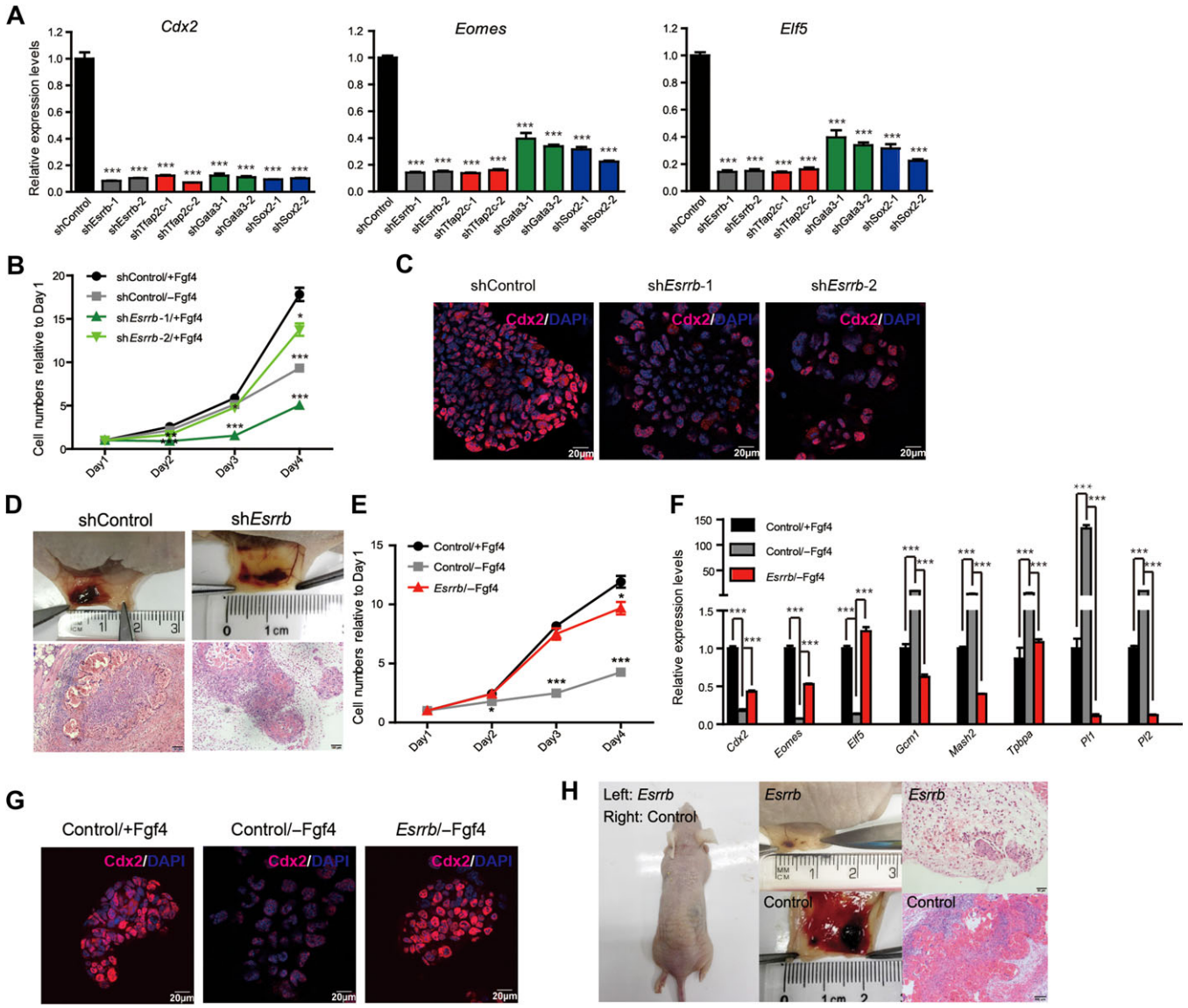

Figure 1 *Esrrb* is critical for maintaining the stem state of TSC. (**A**) qRT-PCR analysis of TSC-specific genes in the indicated shTF-TSCs. The expression levels were normalized to those in shControl-TSCs. (**B**) Kinetics of the cell number during TSC propagation. *Esrrb* deficiency results in a remarkable reduction in cell numbers, which were counted on indicated time points and compared to those on Day 1. (**C**) Immunofluorescent staining of Cdx2 in shControl and two *Esrrb*-KD TSCs. Scale bar, 20 μm. (**D**) Hemorrhagic lesion formation analysis of shControl and *Esrrb*-KD TSCs. The TSCs were subcutaneously injected into immune-deficient nude mice. After 7 days, the formed lesions were analyzed by H&E staining. The shControl-TSC was set as a control. Scale bar, 100 μm. (**E**) Kinetics of the cell number during TSC propagation. Forced expression of *Esrrb* enhances TSC proliferation. The cell numbers were counted on indicated time points and compared to those on Day 1. (**F**) qRT-PCR analysis of TSC-specific genes (*Cdx2*, *Eomes*, and *Elf5*) and differentiation-related genes (*Gcm1*, *Mash2*, *Tpbpa*, *Pl1*, and *Pl2*) in *Esrrb*-overexpressing TSCs after withdraw of Fgf4. Wide-type TSCs cultured with (Control/+Fgf4) or without (Control/−Fgf4) Fgf4 were set as controls. The expression levels were normalized to Control/+Fgf4 TSCs. (**G**) Immunofluorescent staining of Cdx2 in *Esrrb*-overexpressing TSCs after withdraw of Fgf4. The TSCs cultured with or without Fgf4 addition were set as controls. Scale bar, 20 μm. (**H**) Hemorrhagic lesion formation analysis of Control and *Esrrb*-overexpressing TSCs. After 7 days, the formed lesions were analyzed by H&E staining. Scale bar, 100 μm. Data in **A**, **B**, **E**, and **F** are presented as mean ± SEM ($n = 3$). ***$P < 0.001$; **$P < 0.01$; *$P < 0.05$ by ANOVA or Student's *t*-test for comparison.

replaced by artificial maintenance of a high *Esrrb* level. Quantitative analysis showed that *Esrrb* transcript was enriched by more than six times after ectopic expression (Supplementary Figure S1G). Notably, we found that forced expression of *Esrrb* blocked the reported rapid differentiation of TSCs in the absence of Ffg4 (Latos et al., 2015) and further enabled an accelerated proliferation rate (Figure 1E and Supplementary Figure S1H). In addition, *Esrrb* enabled the upregulation of self-renewal markers,

including *Cdx2*, *Eomes*, and *Elf5*, and conversely inhibited the expression of syncytiotrophoblast marker *Gcm1* and spongiotrophoblast markers including *Mash2* and *Tpbpa* (Figure 1F). Besides, immunostaining analysis demonstrated that the downregulated Cdx2 level can be efficiently rescued (Figure 1G). We then accessed the *in vivo* differentiation potential of *Esrrb*-overexpressing TSCs. Interestingly, H&E analysis showed that forced expression of *Esrrb* also restricted the invasion and differentiation ability of TSCs, whereas wild-type TSCs could form typical hemorrhagic lesions in the immune-deficient mice (Figure 1H). Taken together, forced expression of *Esrrb* can keep TSCs in a stem-like state and enable prolonged self-renewal in the absence of Fgf4.

Esrrb can directly target and regulate core TSC regulation network

To gain a deep insight into the underlying mechanism whether and how Esrrb regulates TSC-specific transcriptome and keeps TSCs in a stem state in the absence of Fgf4, we performed RNA-seq analysis on these *Esrrb*-overexpressing TSCs (*Esrrb*/−Fgf4). Meanwhile, TSCs cultured with (Control/+Fgf4) or without Fgf4 (Control/−Fgf4) addition were set as controls (Supplementary Figure S2A). Global expression analysis identified the mass of differentially expressed genes among the three samples, and we then clustered these genes into seven clusters (Supplementary Figure S2A and B). The result indicated that Esrrb could efficiently activate marker genes that are essential for the self-renewal of TSC such as *Cdx2*, *Eomes*, and *Sox2* (Figure 2A; clusters 1 and 5 in Supplementary Figure S2B), which were demonstrated to be downregulated after withdrawal of Fgf4. Besides, Esrrb conversely played a crucial role in inhibiting the upregulated differentiation genes when TSCs were cultured without Fgf4 (clusters 2 and 6). In addition, Esrrb specifically upregulated certain genes which are mainly enriched for mRNA processing, transcription and embryonic development (cluster 7). However, there were still two clusters of genes (clusters 3 and 4) that could not be rescued by *Esrrb* overexpression, which indicated that they might be affected by the Fgf signaling but not regulated and/or targeted by Esrrb.

We next performed chromatin immunoprecipitation followed by high-throughput sequencing (ChIP-seq) analysis to obtain a comprehensive overview of direct targeting regions for Esrrb in TSCs. A significant overlap in target genes was noticed between our data and the public one (Supplementary Figure S2C) (Latos et al., 2015). Motif analysis using MEME/DREME followed by Tomtom suits further indicated that Esrrb peaks were highly enriched in certain known TSC-specific genes. In addition, Esrrb/Esrra-binding motifs were also identified, which implies that Esrrb may have a self-reinforcing function (Supplementary Figure S2D). Besides, those Esrrb-targeting sites in TSCs were predominantly enriched at promoters as well as enhancers (Figure 2B). Importantly, BETA activating/repressive function prediction of the Esrrb from the Esrrb ChIP-seq and RNA-seq data also demonstrated that a great proportion of genes, which were upregulated by *Esrrb* overexpression are more likely to be targeted by Esrrb itself (Figure 2C).

We then analyzed the Esrrb-targeting genes, which were significantly upregulated or downregulated after withdrawal of Fgf4 and could be specifically rescued via *Esrrb* overexpression (Figure 2D and Supplementary Figure S2E). Gene ontology (GO) term analysis further revealed that these upregulated or downregulated Esrrb-targeting genes are both enriched in placental development, blood vessel development, differentiation and cell proliferation processes (Figure 2E). Particularly, Esrrb could target and activate genes which can sustain the self-renewal, promoting cell proliferation; whereas downregulated Esrrb-targeting genes mainly functions in TSC differentiation (Figure 2E). The interactome analysis within these Esrrb-targeting genes showed that the upregulated Esrrb-targeting genes, which included certain core markers in TSCs, exhibited a much closer interaction among each other (Supplementary Figure S2E). These results were further evidenced by a TSC-specific marker gene network analysis, which confirmed that Esrrb could target and activate certain genes including *Cdx2, Eomes*, *Sox2, Fgfr4*, *and Bmp4* (Figure 2F). In contrast, downregulated Esrrb-targeting genes hardly form a strong interaction network (Supplementary Figure S2E). Moreover, the Integrative Genomic Viewer (IGV) analysis also confirmed the enrichment of Esrrb in these loci (Figure 2G). Thus, these results indicate that Esrrb can directly target and regulate predominant TSC-specific makers.

Esrrb is required for the optimal generation of iTSC

Recent studies have shown that ectopic expression of *Gata3*, *Eomes*, *Tfap2c*, and *Myc* (GETM) enables the generation of iTSCs from MEFs (Benchetrit et al., 2015). In our study, we identified that *Esrrb* was progressively upregulated during the iTSC reprogramming and finally maintained a high level in the established iTSCs (Supplementary Figure S3A and B). To test whether Esrrb is essential for iTSC generation, we conducted *Esrrb* depletion by shRNA mediated gene knockdown experiment during the reprogramming process (Figure 3A). The results showed that the efficiency for generating iTSCs was reduced when *Esrrb* was deficient (Figure 3B and Supplementary Figure S3C). Additionally, quantitative analysis in early phase of iTSC reprogramming indicated that depletion of Esrrb prominently inhibited the activation of certain TSC markers, whereas the downregulation of fibroblast-specific marker *Thy1* was not altered (Supplementary Figure S3D). Thus, we concluded that Esrrb is required for the optimal generation of iTSCs.

Esrrb facilitates the conversion of iTSC from MEF

To further identify the role of Esrrb in iTSC generation, *Esrrb* was introduced into MEFs together with lentiviruses carrying GETM (Figure 3A). The result indicated that ectopic expression of *Esrrb* could dramatically increase TSC-like colony numbers by 8–10 times (Figure 3B and Supplementary Figure S3E). Meanwhile, although *Esrrb* could promote the formation of iTSC colonies, it does not obviously shorten the minimal period of time needed to generate these induced cells (Supplementary Figure S3E). Meanwhile, we utilized flow cytometry approach to measure the expression of TSC surface marker CD40 as well as

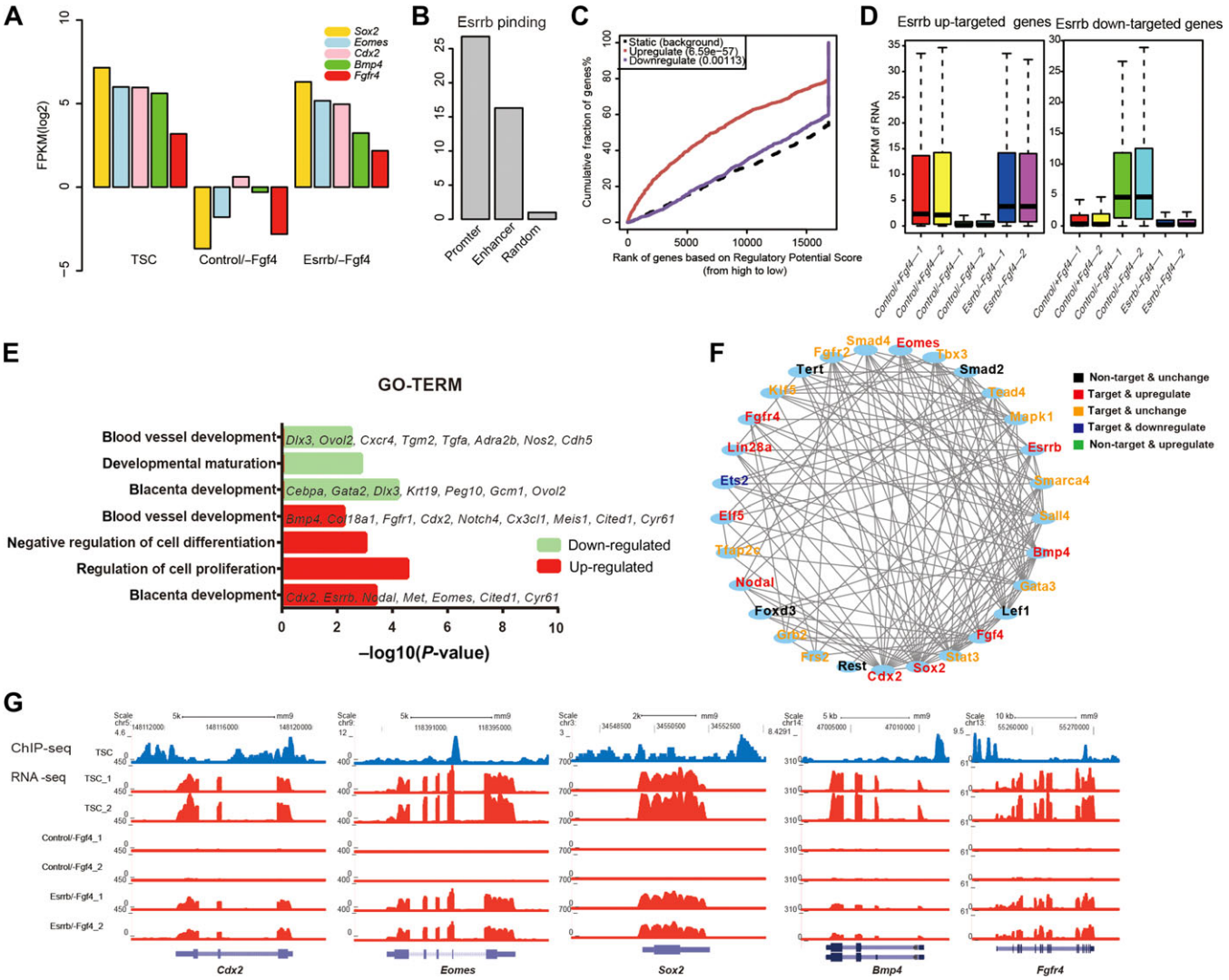

Figure 2 Esrrb acts as a pivotal regulator of the TSC transcriptional network. (**A**) Expression levels of indicated TSC-specific genes in *Esrrb*-overexpressing TSCs (*Esrrb*/–Fgf4) and TSCs cultured with (Control/+Fgf4) or without Fgf4 (Control/–Fgf4). (**B**) The enrichment analysis showed Esrrb-binding sites in promoter and enhancer regions. (**C**) Activating/repressive function prediction of Esrrb from the Esrrb ChIP-seq and RNA-seq data. The red and the purple lines represent the upregulated and downregulated genes, respectively. The dashed line indicates the non-differentially expressed genes as background. (**D**) Expression levels of upregulated and downregulated Esrrb-targeting genes in *Esrrb*-overexpressing TSCs (*Esrrb*/–Fgf4) and TSCs cultured with (Control/+Fgf4) or without Fgf4 (Control/–Fgf4). (**E**) GO analysis of the upregulated (red bars) and downregulated (green bars) Esrrb-targeting genes indicated in **D**. (**F**) Protein–protein interaction network analysis of the reported TSC-specific genes. Esrrb targets and activates certain genes, including *Cdx2*, *Eomes*, *Sox2*, *Fgfr4*, and *Bmp4*. (**G**) IGV analysis of the enrichment of Esrrb at the *Cdx2*, *Eomes*, *Sox2*, *Bmp4*, and *Fgfr4* loci.

MEF surface marker Thy1 during the early stage of the reprogramming process (Rugg-Gunn et al., 2012). The results showed that the percentage of CD40-positive cells increased more rapidly in GETM induction combined with forced expression of *Esrrb* when compared to GETM-only group, whereas the disappearance of Thy1-positive cells was not greatly accelerated (Figure 3C). These findings demonstrate that Esrrb is capable to enhance the GETM-mediated iTSC generation.

Next, we set out to characterize the iTSCs generated by GETM+Esrrb. After 2–3 weeks of induction, TSC-like colonies were picked up and propagated withdraw of doxycycline (Dox), thus the exogenous genes were not induced (Figure 3A). And then, several GETM+Esrrb iTSC lines could be finally established (Figure 3D). The endogenous expression levels of TSC-specific markers *Cdx2* and *Elf5* in the GETM+Esrrb iTSCs were comparable to those in control TSCs and GETM-iTSCs, whereas the MEF-specific gene *Thy1* was not expressed (Figure 3E). Moreover, these iTSCs exhibited typical TSC morphologies and Cdx2 protein level was further confirmed (Figure 3D and Supplementary Figure S3F). Similar to TSCs, these GETM+Esrrb iTSCs could form hemorrhagic lesions with big blood-filled lacunas and differentiated trophoblastic giant cells after subcutaneously

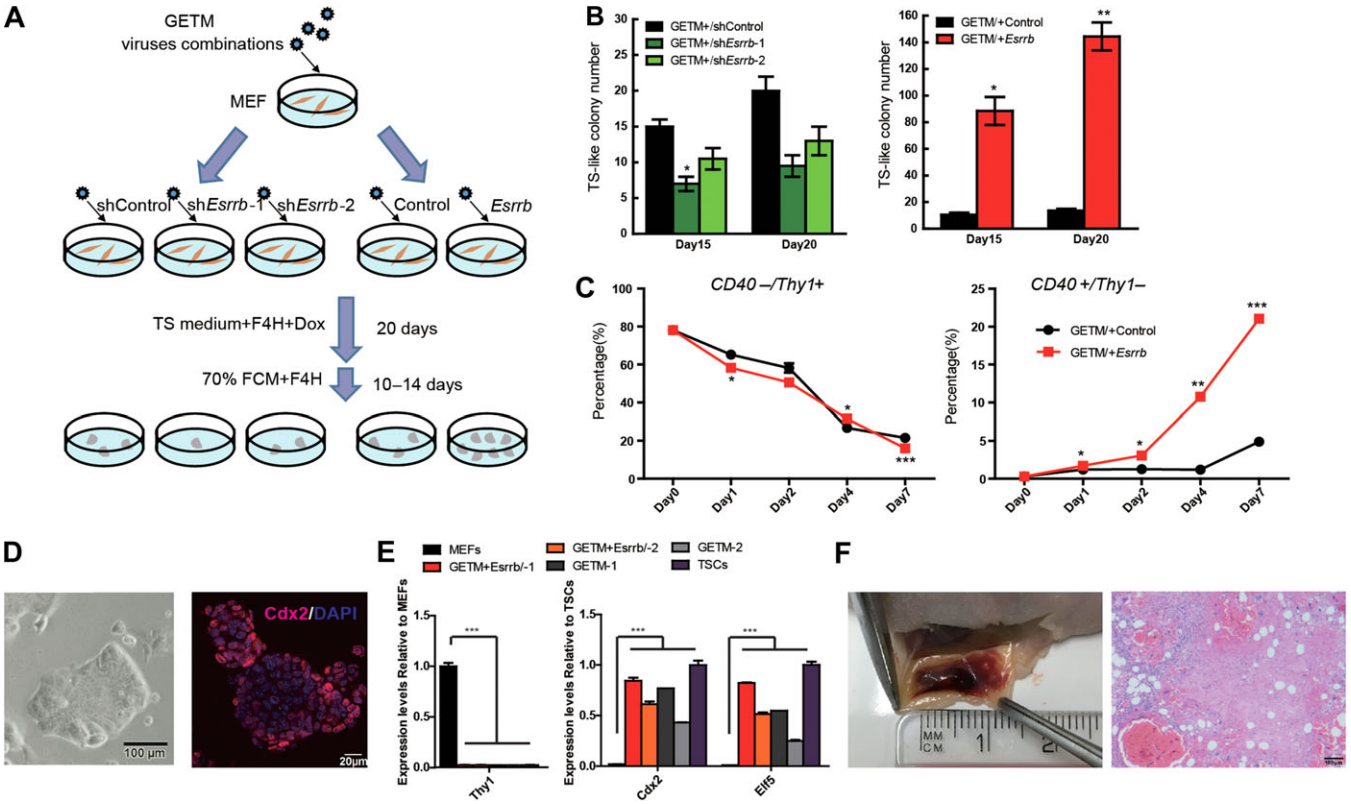

Figure 3 Esrrb facilitates the conversion of iTSCs from MEFs. (**A**) The strategy for functional studies of Esrrb in GETM-mediated generation of iTSCs. (**B**) Analysis of TS-like colony numbers at the indicated days during iTSC generation. *Esrrb* deficiency inhibits the generation of iTSCs (left panel), whereas forced expression of *Esrrb* could facilitate the formation of TS-like colonies (right panel). (**C**) The surface antigen kinetics of iTSC reprogramming showed a gradual loss of Thy1-positive signals (left panel) and a gradual acquisition of CD40-positive signals (right panel). Forced expression of *Esrrb* could promote the enrichment of CD40-positive cells. (**D**) Representative bright field (left panel) and immunofluorescent staining (right panel) images of GETM+Esrrb iTSCs. (**E**) qRT-PCR analysis of Thy1 (left panel), Cdx2, and Elf5 (right panel) in the indicated iTSCs. (**F**) Hemorrhagic lesion formation analysis of GETM+Esrrb iTSCs. Scale bar, 100 μm. Data in **B**, **C**, and **E** are presented as mean ± SEM ($n = 3$). ***$P < 0.001$; **$P < 0.01$; *$P < 0.05$ by ANOVA or Student's *t*-test for comparison.

injected into the immune-deficient nude mice (Figure 3F). To further investigate how Esrrb facilitated the iTSC generation, we monitored the mRNA levels of TSC markers during the reprogramming process. Quantitative analysis revealed that certain Esrrb-targeting TSC-specific markers were activated more rapidly during GETM-mediated reprogramming with forced Esrrb expression (Supplementary Figure S3G). Collectively, these findings demonstrate that Esrrb can facilitate iTSC generation.

Esrrb can replace Eomes to generate iTSCs

As Esrrb could directly active its targeted marker genes and then promote MEF-to-iTSC transition, we aimed to identify whether *Esrrb* could replace one of the four transcriptional factors during iTSC reprogramming. For this purpose, we infected MEFs with lentiviruses carrying *Esrrb* together with any three factors of GETM (Figure 4A). Of note, distinct TSC-like colonies could appear when MEFs were infected with *Esrrb* and ETM or GTM combinations, whereas only GTM+Esrrb iTSC lines (GEsTM-iTSCs) could be successfully established and maintained after Dox withdrawal (Figure 4B and Supplementary Figure S4A). In contrast, no TSC-like colonies and/or iTSC lines could be generated when MEFs were infected by ETM, GTM, GEM, or GET with the control vector under the same culture condition (Figure 4B and Supplementary Figure S4B). Flow cytometry analysis further revealed that CD40-positive cells could be efficiently enriched, accompanied by accelerated downregulation of Thy1-positive cells during GEsTM-mediated reprogramming (Figure 4C). Moreover, RT-qPCR analysis revealed that endogenous TSC-related markers could be quickly reactivated during GEsTM-mediated iTSC generation, which was similar to those observed in GETM-mediated reprogramming (Supplementary Figure S4C).

Quantitative analysis further confirmed the endogenous expression of *Cdx2* and *Elf5* in the GEsTM-iTSCs, which was comparable to those in GETM-iTSCs and canonical TSCs (Figure 4D). In addition, the successfully reactivated Cdx2 protein level in the GEsTM-iTSCs was confirmed by immunostaining as well as western blot analysis (Figure 4E and Supplementary Figure S4D). Moreover, GEsTM-iTSCs could form hemorrhagic lesions when subcutaneously injected into the immune-deficient nude mice, and the differentiated trophoblast cells were further confirmed by

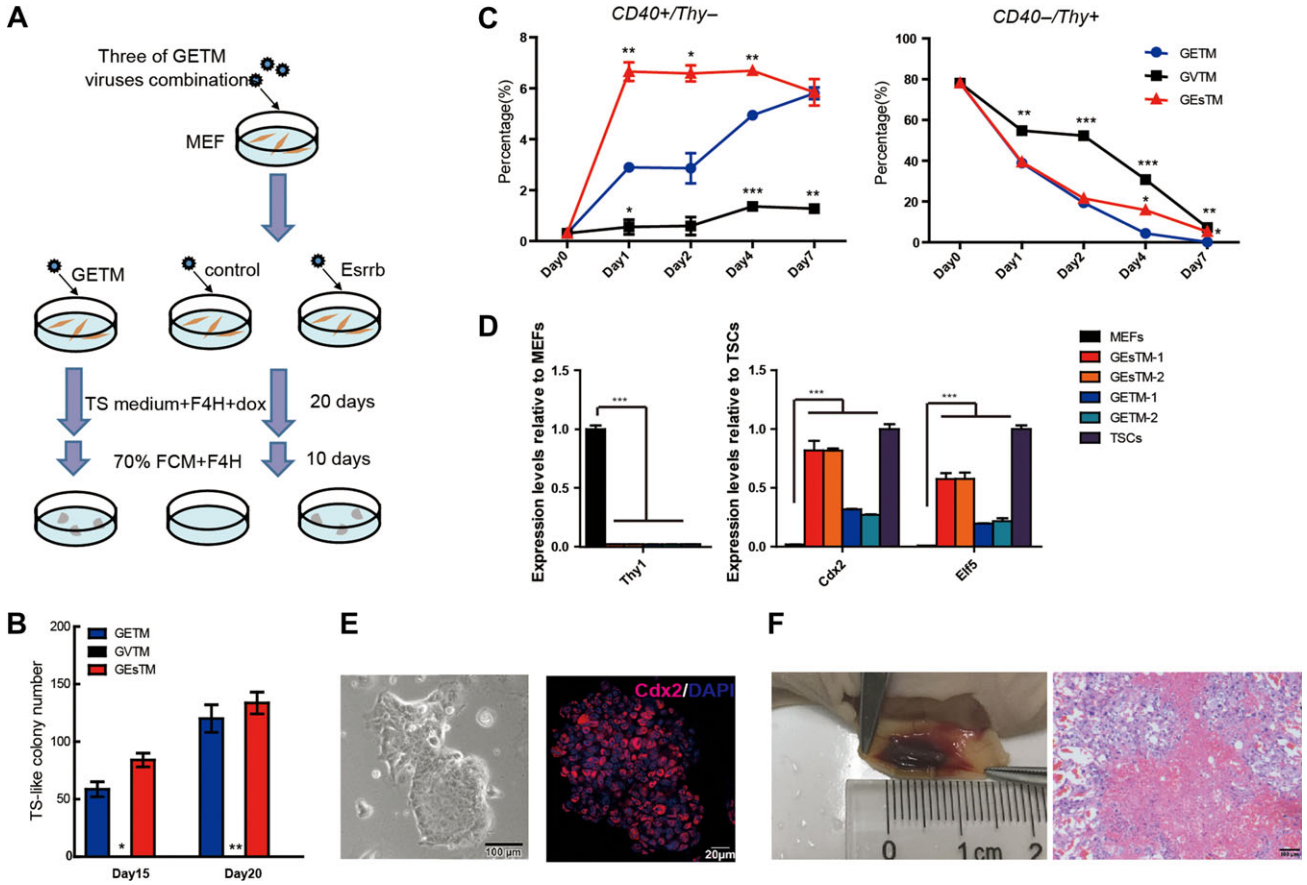

Figure 4 *Esrrb* can replace *Eomes* to generate iTSCs. (**A**) The strategy for GETM replacement by *Esrrb* during iTSC generation. (**B**) Representative TS-like colony numbers at the indicated days during iTSC generation. Parallel experiments were performed among GTEM combination, GTM+Vector (GVTM) combination, and GTM+Esrrb (GEsTM) combination. (**C**) The surface antigen kinetics in GETM-, GVTM-, and GEsTM-mediated iTSC reprogramming. (**D**) qRT-PCR analysis of Thy1 (left panel), Cdx2, and Elf5 (right panel) in the indicated iTSCs. (**E**) Representative bright field (left panel) and immunofluorescent staining (right panel) of Cdx2 in GEsTM-iTSCs. (**F**) Hemorrhagic lesion formation analysis of GEsTM-iTSCs. Scale bar, 100 μm. Data in **B**–**D** are presented as mean ± SEM ($n = 3$). ***$P < 0.001$; **$P < 0.01$; *$P < 0.05$ by ANOVA or Student's *t*-test for comparison.

H&E analysis (Figure 4F). Taken together, these results indicated that *Esrrb* is sufficient to replace *Eomes* and can generate multipotent iTSCs.

Discussion

In this study, we reported that Esrrb is a pivotal regulator in the transcriptional network of TSC and plays a critical role in TSC self-renewal as well as *in vitro* and *in vivo* differentiation. Besides, we demonstrated that ectopic expression of *Esrrb* can efficiently facilitate GETM-mediated iTSC generation from MEF. Moreover, *Esrrb* can substitute for *Eomes* during reprogramming and generate multipotent iTSCs.

Esrrb is a TF, which is previously implicated in ESC self-renewal, and plays a crucial role in maintaining pluripotency by interacting with various other key pluripotent related factors in ESCs (Martello et al., 2012; Papp and Plath, 2012). In multipotent TSCs, Esrrb is reported as a downstream target of Fgf/Mek signaling and can further function in activating numerous TSC-specific genes (Latos et al., 2015). Besides, Esrrb has been demonstrated to be critical for the successful establishment of TSC as well as for the proper development of placentae *in vivo*, whereas its deficiency can cause embryo lethal before E10.5 (Luo et al., 1997). In addition, Esrrb can interact with lysine-specific demethylase Lsd1 and recruit RNAPII, which may further modify chromatin and activate its target transcription in TSC (Latos et al., 2015). Although Esrrb is pivotal to maintain the stem-like state both in TSC and ESC, limited overlap of its bounding sites was noticed, which indicates the function of Esrrb might be divergent in these two kinds of stem cells. Moreover, the function of Esrrb in regulating TSC differentiation ability without Fgf4, as well as in the cell fate conversion, has not yet been carefully elucidated.

In the present study, we aimed to decipher the underlying mechanism whereby Esrrb regulates TSC-specific transcriptome in stem state, differentiation, as well as during reprogramming. Here, several lines of evidence in our study have fully suggested that Esrrb is an essential regulator of the core transcriptional network in TSC. First, *Esrrb* depletion resulted in downregulation

of TSC marker genes and caused rapid differentiation of TSCs albeit they were cultured in Fgf4 containing medium (Figure 1 and Supplementary Figure S1). Besides, *Esrrb*-KD TSCs showed reduced chimeric abilities (Supplementary Figure S1). Second, Esrrb mainly functions in activating marker genes that are essential for the self-renewal of trophoblast such as *Cdx2* and *Eomes*, which are demonstrated to be downregulated after withdrawal of Fgf4 (Figures 1 and 2; Supplementary Figures S1 and S2). As a result, forced *Esrrb* expression can maintain the stem-like state of TSCs when they are cultured without Fgf4 (Figure 1 and Supplementary Figure S1). Third, a great proportion of genes that were upregulated by *Esrrb* overexpression are generally targeted by Esrrb, and those Esrrb-targeting sites in TSCs were predominantly enriched at promoters as well as enhancers (Figure 2 and Supplementary Figure S2). Thus, these results in turn strongly indicate a direct regulation mechanism of Esrrb in TSC.

Recently, ectopic expression of *Gata3*, *Eomes*, *Tfap2c*, and *Myc* (or *Ets2*) was reported to have the ability to reprogram mouse fibroblasts into iTSCs (Benchetrit et al., 2015; Kubaczka et al., 2015). Here, we showed that Esrrb is required for the efficient generation of iTSCs, as its overexpression can further promote GEMT-mediated reprogramming and facilitate the gaining of CD40-positive cells (Figure 3 and Supplementary Figure S3). Besides, this process is accompanied by a prior activation of TSC-related maker genes, which further indicates that Esrrb can directly and positively regulate these Esrrb-targeting TSC markers (Figures 2 and 3; Supplementary Figures S2 and S3). However, depletion of *Esrrb* inhibited the activation of TSC markers and reduced the conversion from MEF to iTSC. Moreover, we confirmed a direct regulation function of Esrrb at the Eomes loci by a factor replacement experiment during iTSC reprogramming (Figure 4 and Supplementary Figure S4). And these GEsTM-iTSCs could be efficiently established, showing typical TSC morphology, expressing TSC-specific marker genes and having *in vivo* differentiation ability.

Taken together, our data demonstrate that Esrrb constitutes the predominant axis controlling both stem state maintenance and differentiation of TSC and is important for the generation of iTSC.

Materials and methods

Mice and cell culture

All mouse experiments were performed in accordance with the University of Health Guide for the Care and Use of Laboratory Animals and were approved by the Biological Research Ethics Committee of Tongji University. The specific pathogen-free mice were housed in the animal facility of Tongji University. Mouse were housed under a 12-h light/dark cycle under pathogen-free conditions at 22°C ± 2°C and fed with free access to standard mouse chow and tap water.

MEFs were derived from 13.5 dpc (days postcoitum) embryos that were collected from female Oct4-green fluorescent protein (GFP) transgenic mice mated with male Rosa26-M2rtTA mice. RO-7 TSCs, which was generated in our laboratory and published before (Wu et al., 2011), were cultured in 70% feeder condition medium (FCM)+heparin (F4H) medium composed of 30% TS medium (TSM; RPMI1640 supplemented with 20% FBS, 1 mM sodium pyruvate, 100 μM β-mercaptoethanol, 2 mM L-glutamine), 70% FCM, 25 ng/ml Fgf4, and 1 μg/ml F4H. For Fgf4 withdraw experiments, Fgf4 was totally removed from culture medium.

Plasmid construction and generation of Esrrb overexpression and knockdown TSCs

The dox inducible FUW-TetO-Gata3, -Eomes, -Tfap2c, and -Esrrb were constructed by introducing the coding sequence of each factor into the FUW-tetO vector. The FUW-TetO-cMyc plasmid was generously provided by Dr Rudolf Jaenisch's laboratory at the Whitehead Institute for Biomedical Research.

The *Esrrb* overexpression plasmid was generated by cloning the open reading frame of *Esrrb* and inserted into the pEF1aFLBIO-puro expression vector. Transfections were performed for 4–5 h in Opti-MEM media supplemented with Fgf4 and heparin using 1% Lipofectamine 2000 (Life Technologies) and then changed to TSC culture medium. After 24 h, cells were selected with 1 μg/ml puromycin. The colonies were individually picked, propagated, and tested for the expression of exogenous *Esrrb*. Then the stable *Esrrb*-overexpressing TSCs could be established.

For the gene knockdown assay in TSCs, the wide-type TSCs were infected with *Esrrb* shRNA viruses (sh#1 or sh#2) or the scramble shRNA (shCtrl) virus, respectively. The *Esrrb*-KD stable cell lines could be enriched by fluorescence-activated cell sorting (FACS). The *Esrrb* shRNAs and scramble sequences are listed in Supplementary Table S1.

Generation of iTSCs

The procedure of iTSCs derivation was described previously (Benchetrit et al., 2015). Briefly, 293T cells were transfected by Vigofect (Vigorous Biotechnology) with the FUW-TetO vectors with the packaging plasmids psPAX2 and pMD2.G (5:3:2). The medium was replaced 12 h after transfection, and virus-containing supernatant was collected after 48, 60, and 72 h. MEFs at the third passage were cultured in 35-mm dishes at a density of 5×10^4 cells/dish and were incubated with filtered viral supernatants filtered through a 0.45-mm filter (Merk Millipore) containing 8 μg/ml polybrene (Merk Millipore). The medium was replaced with fresh DMEM (Life Technologies) supplemented with 10% (*v*/*v*) FBS (Gibco) and 1 mM L-glutamine (Life Technologies) after third infection. After 18 h culture, medium was replaced with TSM+F4H medium supplemented with 2 μg/ml doxycycline (Dox) (Sigma). The medium was replaced every day until the trophoblast stem-like colonies appeared. The cells were cultured for another 10 days with TSC culture cell medium without doxycycline, and then the colonies were picked and propagated.

Flow cytometric analysis of CD40 and Thy1 expression

Cells were harvested with 0.05% trypsin/EDTA (Gibco), resuspended in FACS buffer (1% FBS in PBS) and filtered through a 40-mm cell strainer. About 100000 cells were incubated with

0.4 mg/ml anti-CD40 antibody (R&D systems) and PE/Cy7 anti-CD90.2 (Thy1.2) antibody (Biolegend) for 30 min on ice. Cells were then washed with FACS buffer, resuspended in FACS buffer with anti-goat Alexa-488 antibody, and incubated for 20 min on ice in the dark. After washing, cells were resuspended in FACS buffer. Staining was acquired on a FACSCanto (BD Biosciences) and analyzed using FlowJo Software (Tree Star). *P*-values were calculated using one-way ANOVA.

Reverse transcription and quantitative real-time PCR

Total RNA was extracted using Trizol reagent (Invitrogen) and reversely transcribed using 5× All-In-One RT MasterMix (ABM) according to the manufacturer's recommendations. Quantitative RT-PCR was performed using a SYBR Premix Ex Taq II (TaKaRa), and signals were detected with an ABI7500 Real Time PCR System (Applied BioSystems). All samples were run in triplicate. *Gapdh* was used as an endogenous control. All the primers used were synthetized in Sangon Biotech Co., Ltd and listed in Supplementary Table S2.

Immunofluorescent staining

Cells were fixed with 4% paraformaldehyde (Sangon Biotech) for 15 min and then permeabilized with 0.2% Triton X-100 for 15 min at room temperature (RT). The samples were blocked with 2.5% BSA (Sigma) for 1 h and then incubated with the primary antibodies Cdx2 (1:500, Abcam) overnight at 4°C. After washing three times with PBS, the samples were incubated with the appropriate secondary antibody at for 45 min. The nuclei were stained with DAPI (Life Technologies). All stained samples were observed using a NIKON ECLIPSE 80i microscope (Nikon Instruments Inc.).

Western blot

Cells and tissues were lysed by cold RIPA buffer. The supernatants were harvested and protein concentration was determined by the Enhanced BCA Protein Assay Kit (Beyotime). The lysates were then separated by 10% SDS-PAGE and transferred electrophoretically onto polyvinylidene difluoride membranes. After blocked with 5% non-fat milk in TBST, membranes were incubated with the primary antibodies against Cdx2 (Abcam), Gapdh (Proteintech), or α-Tubulin (Proteintech). After incubation with an HRP-conjugated secondary antibody (Life Technology), the signals were measured by using ECL reagents (Tanon). Gapdh or α-Tubulin was used as an endogenous loading control.

Hemorrhagic lesion formation and H&E analysis

The hemorrhagic lesion formation analysis was performed as previously reported (Kubaczka et al., 2014). In brief, 3×10^6 TSCs or iTSCs were re-suspended in 200 μl 70% FCM+F4H medium and were subcutaneously injected into adult female nude mice. Seven days after post-injection, the lesions were dissected, fixed in 4% paraformaldehyde overnight, embedded in paraffin, and sectioned (4 μm), followed by H&E staining. The H&E staining was performed at the Shanghai Yichang Biosciences Co., Ltd.

RNA-seq

Total RNA was isolated from cell pellets by Trizol reagent (TaKaRa) and RNA-Seq library were generated using KAPA Strandard mRNA-Seq Kits (KK8420) according to the manufacturer's recommendations. Paired-end 125-bp sequencing was performed on HiSeq 2500 system (Illumina) at Berry Genomics Corporation.

Esrrb ChIP-seq analysis

Esrrb-overexpressing TSCs were resuspended in lysis buffer and chromatin was sonicated to 200–500 bp with Covaris M220 system. Then, the sonicated chromatin was immunoprecipitated with the antibodies. ChIP DNA was reverse-crosslinked, eluted, and purified by phenol–chloroform–isoamyl alcohol extraction, followed by ethanol precipitation. We performed two independent IP reactions for each sample, and ChIP DNA was pooled for library preparation following the KAPA Hyper Prep Kit (KK8504) protocol. Paired-end 125-bp sequencing was performed on HiSeq 2500 system (Illumina) at Berry Genomics Corporation.

Statistics

Student's *t*-test, one-way ANOVA, and Fisher's exact test were performed for statistical comparisons.

ChIP-seq and RNA-seq data processing

ChIP-seq data for Esrrb were obtained from *Esrrb*-overexpressing TSCs. Public Esrrb and control ChIP-seq data were downloaded from EMBL database (accession number: E-MTAB-3565). All ChIP-seq data were aligned using the bowtie2 v2.2.3 (Langmead and Salzberg, 2012) default command on the mouse genome version mm9. Signal tracks for each sample were generated using the MACS2 v2.1.0 (Zhang et al., 2008) pileup function and were normalized to 1 million reads for downstream analysis. The RNA-seq reads were mapped to the mm9 reference genome using TopHat v2.0.12 (Trapnell et al., 2009). Expression level for each gene was quantified to reads counted by GFOLD v1.1.3 (Feng et al., 2012) count command. Expression level for each gene was quantified to FPKM by Cufflinks v2.2.1 (Trapnell et al., 2010). The replicate for each state was averaged, as they were highly reproducible with each other. Differentially expressed genes were identified by GFOLD diff command, setting GFOLD cutoff to ±1, respectively. We identified target genes with ChIP-seq data and RNA-seq data by BETA v1.0.7 (Wang et al., 2013) minus and basic command.

Data visualizing

Peak signal of Esrrb and expression signal of target genes were visualized on UCSC Genome browser (http://genome.ucsc.edu/). Figures were visualized with a custom R script using different packages and commands.

Motif analysis

The motif analysis was performed using motif-based sequence analysis tools MEME v4.10.0 (Bailey and Elkan, 1994) and TOMTOM v4.10.0 (Gupta et al., 2007). The regions of Esrrb peaks center ± 25 base pairs were extracted, and the minimum overlap between query and target is 5.

Network analysis

For interactome analysis, the significant Esrrb-correlated genes were uploaded to STRING v10.0 (http://string-db.org/) (Szklarczyk et al., 2015) to identify their interactions. The generated network text file was visualized and categorized using Cytoscape v3.4.0 (Shannon et al., 2003).

GO analysis

Functional annotation was performed using the Database for Annotation, Visualization and Integrated Discovery (DAVID) (Huang et al., 2009) Bioinformatics Resource v6.7. GO terms for each functional cluster were summarized to a representative term, and *P*-values were plotted to show the significance.

Accession number

The gene expression omnibus (GEO) accession number for the RNA-seq data and ChIP-seq analyses in this paper is GSE104696.

Supplementary material

Supplementary material is available at *Journal of Molecular Cell Biology* online.

Acknowledgements

We are grateful to our colleagues in the laboratory for their assistance with the experiments and in the preparation of this manuscript.

Funding

This work was primarily supported by the National Key R&D Program of China (2016YFA0100400) and the National Natural Science Foundation of China (31721003). This work was also supported by the Ministry of Science and Technology of China (2015CB964800, 2015CB964503, and 2018YFA0108900), the National Natural Science Foundation of China (81630035, 31871446, and 31771646), the Shanghai Rising-Star Program (17QA1404200), the Shanghai Chenguang Program (16CG17), the Shanghai Municipal Medical and Health Discipline Construction Projects (2017ZZ02015), National Postdoctoral Program for Innovative Talents (BX201700307), and China Postdoctoral Science Foundation (2017M621527).

Conflict of interest: none declared.

Author contributions: H.G., R.G., and L.Z. contributed to collection and/or assembly of data, data analysis and interpretation, and manuscript writing. W.X. and Y.Z. contributed to computational analysis. R.Z. and H.W. contributed to provision of study materials and data analysis and interpretation. J.C., Y.G., and S. G. contributed to conception and design, financial support, manuscript writing, and final approval of the manuscript.

References

Adachi, K., Nikaido, I., Ohta, H., et al. (2013). Context-dependent wiring of Sox2 regulatory networks for self-renewal of embryonic and trophoblast stem cells. Mol. Cell *52*, 380–392.

Auman, H.J., Nottoli, T., Lakiza, O., et al. (2002). Transcription factor AP-2 gamma is essential in the extra-embryonic lineages for early postimplantation development. Development *129*, 2733–2747.

Bailey, T.L., and Elkan, C. (1994). Fitting a mixture model by expectation maximization to discover motifs in biopolymers. Proc. Int. Conf. Intell. Syst. Mol. Biol. *2*, 28–36.

Benchetrit, H., Herman, S., van Wietmarschen, N., et al. (2015). Extensive nuclear reprogramming underlies lineage conversion into functional trophoblast stem-like cells. Cell Stem Cell *17*, 543–556.

Cambuli, F., Murray, A., Dean, W., et al. (2014). Epigenetic memory of the first cell fate decision prevents complete ES cell reprogramming into trophoblast. Nat. Commun. *5*, 5538.

Cockburn, K., and Rossant, J. (2010). Making the blastocyst: lessons from the mouse. J. Clin. Invest. *120*, 995–1003.

Donnison, M., Beaton, A., Davey, H.W., et al. (2005). Loss of the extraembryonic ectoderm in Elf5 mutants leads to defects in embryonic patterning. Development *132*, 2299–2308.

Feng, J.X., Meyer, C.A., Wang, Q., et al. (2012). GFOLD: a generalized fold change for ranking differentially expressed genes from RNA-seq data. Bioinformatics *28*, 2782–2788.

Georgiades, P., and Rossant, J. (2006). Ets2 is necessary in trophoblast for normal embryonic anteroposterior axis development. Development *133*, 1059–1068.

Gupta, S., Stamatoyannopoulos, J.A., Bailey, T.L., et al. (2007). Quantifying similarity between motifs. Genome Biol. *8*, R24.

Huang, D.W., Sherman, B.T., and Lempicki, R.A. (2009). Bioinformatics enrichment tools: paths toward the comprehensive functional analysis of large gene lists. Nucleic Acids Res. *37*, 1–13.

Kubaczka, C., Senner, C., Arauzo-Bravo, M.J., et al. (2014). Derivation and maintenance of murine trophoblast stem cells under defined conditions. Stem Cell Reports *2*, 232–242.

Kubaczka, C., Senner, C.E., Cierlitza, M., et al. (2015). Direct induction of trophoblast stem cells from murine fibroblasts. Cell Stem Cell *17*, 557–568.

Kunath, T., Strumpf, D., and Rossant, J. (2004). Early trophoblast determination and stem cell maintenance in the mouse—a review. Placenta *25*, S32–S38.

Langmead, B., and Salzberg, S.L. (2012). Fast gapped-read alignment with Bowtie 2. Nat. Methods *9*, 357–U354.

Latos, P.A., Goncalves, A., Oxley, D., et al. (2015). Fgf and Esrrb integrate epigenetic and transcriptional networks that regulate self-renewal of trophoblast stem cells. Nat. Commun. *6*, 7776.

Latos, P.A., and Hemberger, M. (2014). Review: the transcriptional and signalling networks of mouse trophoblast stem cells. Placenta *35*, S81–S85.

Luo, J.M., Sladek, R., Bader, J.A., et al. (1997). Placental abnormalities in mouse embryos lacking the orphan nuclear receptor ERR-β. Nature *388*, 778–782.

Martello, G., Sugimoto, T., Diamanti, E., et al. (2012). Esrrb is a pivotal target of the Gsk3/Tcf3 axis regulating embryonic stem cell self-renewal. Cell Stem Cell *11*, 491–504.

Odiatis, C., and Georgiades, P. (2010). New insights for Ets2 function in trophoblast using lentivirus-mediated gene knockdown in trophoblast stem cells. Placenta *31*, 630–640.

Okae, H., Toh, H., Sato, T., et al. (2018). Derivation of human trophoblast stem cells. Cell Stem Cell *22*, 50–63.e6.

Papp, B., and Plath, K. (2012). Pluripotency re-centered around Esrrb. EMBO J. *31*, 4255–4257.

Ralston, A., Cox, B.J., Nishioka, N., et al. (2010). Gata3 regulates trophoblast development downstream of Tead4 and in parallel to Cdx2. Development *137*, 395–403.

Ralston, A., and Rossant, J. (2006). How signaling promotes stem cell survival: trophoblast stem cells and Shp2. Dev. Cell *10*, 275–276.

Roberts, R.M., and Fisher, S.J. (2011). Trophoblast stem cells. Biol. Reprod. *84*, 412–421.

Rugg-Gunn, P.J., Cox, B.J., Lanner, F., et al. (2012). Cell-surface proteomics identifies lineage-specific markers of embryo-derived stem cells. Dev. Cell *22*, 887–901.

Russ, A.P., Wattler, S., Colledge, W.H., et al. (2000). Eomesodermin is required for mouse trophoblast development and mesoderm formation. Nature *404*, 95–99.

Shannon, P., Markiel, A., Ozier, O., et al. (2003). Cytoscape: a software environment for integrated models of biomolecular interaction networks. Genome Res. *13*, 2498–2504.

Sozen, B., Amadei, G., Cox, A., et al. (2018). Self-assembly of embryonic and two extra-embryonic stem cell types into gastrulating embryo-like structures. Nat. Cell Biol. *20*, 979–989.

Strumpf, D., Mao, C.A., Yamanaka, Y., et al. (2005). Cdx2 is required for correct cell fate specification and differentiation of trophectoderm in the mouse blastocyst. Development *132*, 2093–2102.

Szklarczyk, D., Franceschini, A., Wyder, S., et al. (2015). STRING v10: protein-protein interaction networks, integrated over the tree of life. Nucleic Acids Res. *43*, D447–D452.

Tanaka, S., Kunath, T., Hadjantonakis, A.K., et al. (1998). Promotion of trophoblast stem cell proliferation by FGF4. Science *282*, 2072–2075.

Trapnell, C., Pachter, L., and Salzberg, S.L. (2009). TopHat: discovering splice junctions with RNA-Seq. Bioinformatics *25*, 1105–1111.

Trapnell, C., Williams, B.A., Pertea, G., et al. (2010). Transcript assembly and quantification by RNA-Seq reveals unannotated transcripts and isoform switching during cell differentiation. Nat. Biotechnol. *28*, 511–U174.

Tremblay, G.B., Kunath, T., Bergeron, D., et al. (2001). Diethylstilbestrol regulates trophoblast stem cell differentiation as a ligand of orphan nuclear receptor ERRβ. Genes Dev. *15*, 833–838.

Wang, C.F., Liu, X.Y., Gao, Y.W., et al. (2018). Reprogramming of H3K9me3-dependent heterochromatin during mammalian embryo development. Nat. Cell Biol. *20*, 620–631.

Wang, S., Sun, H.F., Ma, J., et al. (2013). Target analysis by integration of transcriptome and ChIP-seq data with BETA. Nat. Protoc. *8*, 2502–2515.

Wen, F., Tynan, J.A., Cecena, G., et al. (2007). Ets2 is required for trophoblast stem cell self-renewal. Dev. Biol. *312*, 284–299.

Werling, U., and Schorle, H. (2002). Transcription factor gene AP-2 gamma essential for early murine development. Mol. Cell. Biol. *22*, 3149–3156.

Wu, T., Wang, H., He, J., et al. (2011). Reprogramming of trophoblast stem cells into pluripotent stem cells by Oct4. Stem Cells *29*, 755–763.

Yamamoto, H., Flannery, M.L., Kupriyanov, S., et al. (1998). Defective trophoblast function in mice with a targeted mutation of Ets2. Genes Dev. *12*, 1315–1326.

Zhang, Y., Liu, T., Meyer, C.A., et al. (2008). Model-based Analysis of ChIP-Seq (MACS). Genome Biol. *9*, R137.